Systems & Control Transactions

Original Research Article
Peer Reviewed Conference Proceeding
ESCAPE 36 - European Symposium on Computer Aided Process Engineering
Sheffield, UK. 21-24 June 2026

PSE PRESS

Optimization-based design of distillation processes with embedded pressure drop and HETP correlations

Sina Bertram[a], Jonas Schnurr[a], and Mirko Skiborowski[a]*

[a] Hamburg University of Technology, Institute of Process Systems Engineering, Hamburg, Germany
* Corresponding Author: mirko.skiborowski@tuhh.de.

ABSTRACT

To improve the energy efficiency of distillation processes, various process intensification concepts have been proposed, including direct heat integration and thermal coupling. Identifying the most suitable alternative for a given separation task requires a rigorous and consistent techno-economic optimization. Superstructure models typically rely on isobaric operation and fixed HETP values, in order to avoid treating column hydraulics when solving the already challenging mixed-integer nonlinear optimization problems. In order to overcome this limitation and evaluate the effect of the simplification, the current work extends a rigorous equilibrium-stage superstructure model to account for tray-specific pressure drop and HETP values. A polylithic solution approach is implemented to improve the convergence for the resulting optimization problems. The proposed approach is demonstrated for the optimization of heat-integrated distillation sequences operated at close to atmospheric and vacuum conditions, enabling a closer investigation of the impact of the classically applied simplifications. As the results illustrate that the overall energy demand and total annualized costs are only marginally affected for the considered wide-boiling mixtures the evaluation of competing process configurations will not be affected by the simplifications. However, considerable changes in column height and heat exchanger areas are observed, particularly under vacuum operation, such that column hydraulics should be considered in design optimization, in case column size restrictions or other considerations require a more accurate equipment sizing.

Keywords: Distillation, Energy integration, Superstructure, Optimization, Pressure drop

INTRODUCTION

Distillation remains the most widely applied separation technology in the chemical and process industries, accounting for approximately 90-95% of all fluid separations tasks [1] and a substantial share of the overall industrial energy demand. Despite its high energy consumption, direct substitution of distillation by alternative separation technologies is largely impractical due to its broad applicability, wide throughput range and capability to produce multiple high-purity products within a single unit [2]. In the context of rising energy prices and increasingly stringent environmental regulations, the development of energy-efficient distillation processes is therefore of central importance.

Numerous energy integration concepts have been proposed and demonstrated as effective means to reduce energy demand [3]. One prominent approach is direct heat integration between columns, in which the heat of condensation of the top vapor from one column is used to supply the heat for evaporating part of the bottoms stream of another column. This is achieved by adjusting the operating pressure of at least one column such that the top temperature of the heat-supplying column exceeds the bottom temperature of the heat-receiving column [4]. For two columns with comparable heat duties, direct heat integration has the potential to reduce energy consumption by up to 50% [4].

Another option to reduce the energy requirement of distillation processes is thermal coupling in which heat exchangers and liquid streams between adjacent distillation columns are replaced by bidirectional liquid and vapor transfer. Equipment-integrated dividing wall column (DWC) implement thermally coupled columns in a single shell and have been shown to reduce capital cost by approximately 30% compared to conventional, non-

integrated distillation sequences [5].

The identification of the best performing concept requires a systematic evaluation of all available process configurations. However, performing a detailed and rigorous analysis of all alternatives with rigorous models is usually intractable, such that shortcut models are the preferred choice for an initial screening [6]. Even the separation of nonideal mixtures can be addressed effectively when making use of thermodynamically sound pinch-based methods [7]. Yet this screening provides only an estimate of the performance, mandating that the most promising alternatives are further evaluated by more rigorous models and a techno-economic assessment.

The optimal design of distillation processes can be determined either through simulation-based approaches or via rigorous numerical optimization [8]. Simulation-based approaches can readily account for column hydraulics, as the column design, especially the number of stages in each section, are fixed prior to simulation. However, typically applied sequential optimization methods are rather cumbersome [5, 9], while gradient-free optimization using surrogate models with response surface methodologies [10] become computationally expensive when design spaces are large.

Mathematical programming applied to superstructure models posed as mixed-integer nonlinear programming (MINLP) problems enable a simultaneous design of the column structure and operating conditions building on gradient-based optimization [5, 8, 11]. While this approach allows for proven (local) optimality, the reported models usually build on isobaric conditions and constant height equivalent of a theoretical plate (HETP) values. Incorporating column hydraulics for pressure drop is a challenge as the actual number of stages and column dimensions are decision variables. Pressure variations resulting from friction losses along the column height affect the boiling temperature, relative volatilities, and ultimately separation performance [12]. Additionally, the pressure drop can increase the heating and cooling demands, and influence the relationship between the number of stages and energy demand, which may become nonlinear at higher stage numbers [13]. In direct heat-integrated distillation sequences, changes in pressure directly impact the reboiler temperature and, consequently, the available temperature driving force in the integrated heat exchanger, thereby significantly influencing feasibility and efficiency. For DWCs, the pressure drop in the parallel sections impacts the vapor split below the dividing wall and thus potentially impairs operation at minimum energy demand.

Although the common simplifications improve the numerical solution of the resulting MINLP problems, they may impair the identification of feasible/optimal designs and may bias the comparison of different process alternatives. While some recent studies have incorporated pressure drop correlations into rigorous distillation models [14] or superstructure optimization of retrofit problems with fixed column dimensions [15], the direct consideration of pressure drop and HETP correlations in superstructure-based design optimization with unknown column dimensions has not been addressed.

Therefore, the current work presents a proof of concept by extending an existing superstructure-based design optimization [16-19] by incorporating correlations for pressure drop and HETP as functions of the vapor load, expressed via the F-factor. By accounting for these effects at the conceptual design stage, a more realistic evaluation of energy-integrated distillation processes is enabled. Furthermore, an investigation of the impact of these correlations on the optimal design is investigated for representative case studies on the design of a heat integrated direct sequence for the separation of two wide boiling mixtures at vacuum and close to atmospheric conditions.

METHODOLOGY

In this work, a rigorous techno-economic optimization is preformed using an equilibrium-stage superstructure model based on the MESH equations and implemented in the General Algebraic Modeling System (GAMS). The resulting MINLP problem is solved as a series of successively relaxed NLP problems [16]. The following subsections describe the superstructure model for individual distillation columns, its extension to directly heat-integrated sequences, as well as the modifications for the implementation of pressure drop and HETP correlations.

Superstructure model for individual distillation columns

The superstructure model for an individual distillation column and its implementation is illustrated in **Figure 1.** It builds on the initial work of Kraemer et al. [16] and Skiborowski et al. [17], which was inspired by the work of Bartttfeld et al. [11]. The sizing of the stripping and rectifying sections is enabled by variable locations for the feed, reflux and boil-up streams. Stages above the reflux and below the boil-up tray are effectively bypassed and do not contribute to the separation. They are consequently not considered for equipment sizing and cost calculations.

Each equilibrium stage is described by the MESH equations, comprising mass balances, vapor-liquid equilibrium relations, summation constraints, and enthalpy balances. The thermodynamic properties and vapor-liquid equilibrium calculations are modeled via external equations implemented via a dynamic link library (DLL), enabling a reduced-space formulation that significantly decreases the number of variables and equations

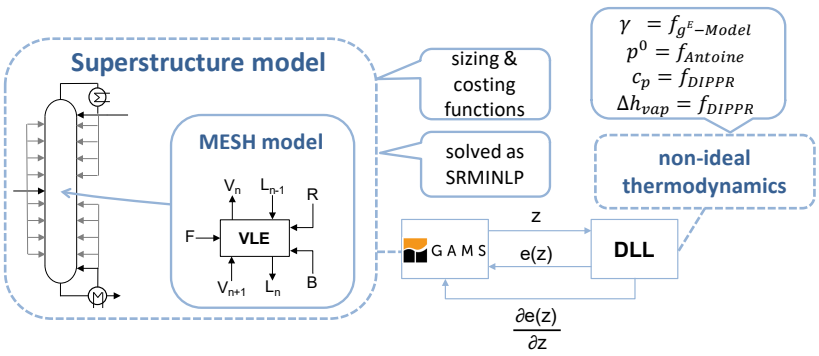

Figure 1. Superstructure model of an individual distillation column and implementation in GAMS with external equations for VLE computations.

managed by GAMS [17].

The optimization objective is to minimize the total annualized cost (TAC). Utility prices are derived from Turton et al. [20], while equipment costs are estimated using Guthrie's method, as outlined by Biegler et al. [21].

Modeling of direct heat-integrated sequences

The model of the heat-integrated direct sequence is based on the work of Waltermann and Skiborowski [18] with the adaptions described by Adami et al. [19]. The operating pressure of the second column is determined from a pre-defined approach temperature and flash calculations for the bottom stream of the first column and top vapor of the second column. Depending on the individual heat requirements either an additional condenser for the second column or an additional reboiler for the first column is implemented to compensate for a mismatch, while an intermediate heat exchanger provides the necessary heat to reach saturation conditions for the connecting stream at the increased pressure.

Pressure drop and HETP correlations

While the columns were considered isobaric in all preceding work on optimization-based design, the current work employs pressure drop and HETP correlations as functions of the vapor load, represented by the F-factor

$$FF_n = u_n^{superficial} \cdot \sqrt{\rho_n^{vapor}} = \frac{4 \cdot \dot{V}_n}{\pi \cdot D_{Col}^2} \cdot \sqrt{\frac{R \cdot T_n \cdot \sum_i y_{i,n} \cdot M_i}{p_n}}, \quad (1)$$

following the retrofit design approach described by Horsch et al. [15]. The column diameter is determined by the maximum vapor load across all active stages, excluding condenser and reboiler stages, following Douglas correlation [22]

$$D_{Col} \geq \sqrt{\frac{4 \cdot \dot{V}_n}{\pi \cdot FF_n}} \cdot \sqrt{\frac{R \cdot T_n \cdot \sum_i y_{i,n} \cdot M_i}{p_n}}, n = 2, \dots, n_{max} - 1. \quad (2)$$

The actual column diameter is considered to be the largest required stage diameter, ensuring that the maximum allowable F-factor is not exceeded

$$FF_n \leq FF_{max}, n = 2, \dots, n_{max} - 1. \quad (3)$$

The pressure drop per height and the HETP of the individual stages are estimated using polynomial correlations, which are fitted to vendor data for Sulzer BX structured packing derived at 960 mbar [23]:

$$\left(\frac{\Delta p}{h}\right)_n = \left(1 + b_{R,n} - \sum_{m=n+1}^{n_{max}} b_{R,m} + \sum_{m=1}^{n-1} b_{B,m}\right) \cdot (0.3617 \cdot FF_n^3 - 0.6838 \cdot FF_n^2 + 0.7572 \cdot FF_n) \quad (4)$$

$$HETP_n = \left(1 - \sum_{m=n+1}^{n_{max}} b_{R,m} + \sum_{m=1}^{n-1} b_{B,m}\right) \cdot (0.0120 \cdot FF_n^3 - 0.0666 \cdot FF_n^2 + 0.1657 \cdot FF_n + 0.0872) \quad (5)$$

Stages that are effectively bypassed by either the reflux or the boil-up stream do not contribute to the separation performance, as either the liquid or vapor stream is zero, such that the mass- and energy balance enforce the same for the liquid or vapor stream leaving the stage [16]. In order to maintain this property and implement the stage-specific pressure drop and HETP, the values of the bypassed stages are also set to zero, by accounting for the binary decision variables of the reflux ($b_{R,n}$) and boil-up ($b_{B,n}$) location as listed in eq. (4) and (5).

In context of the condenser stage ($b_{R,n} = 1$) and the reboiler stage (n_{max}), a doubled pressure drop is assumed to account for the effects of additional friction and phase change in the heat exchangers

$$p_{n_{max}} = p_{n_{max}-1} + 2 \cdot \left(\sum_{m=1}^{n_{max}} b_{B,m} \cdot \frac{\Delta p}{h}_m\right) \cdot \left(\sum_{m=1}^{n_{max}} b_{B,m} \cdot HETP_m\right). \quad (6)$$

The resulting pressure profile along the column is computed recursively as

$$p_n = p_{n-1} + \left(\frac{\Delta p}{h}\right)_n \bullet HETP_n, n = 2, \ldots, n_{max} - 1. \quad (7)$$

In the current work the pressure at the condenser is fixed at the operating pressure, which is determined by means of a preceding shortcut calculation. However, this constraint could also be relaxed to allow for further improvements.

Initialization and solution procedure

The resulting MINLP problem is solved using a successively relaxed continuous reformulation approach, as outlined by Kraemer et al. [16]. The binary decision variables are relaxed and discrete values are successively enforced through penalty terms based on the Fischer-Burmeister functions. To enhance numerical robustness, a polylithic solution strategy (cf. **Figure 2**) is employed following the concept described by Waltermann and Skiborowski [18].

After a first initialization of the individual column models using all available stages (with fixed reflux and boil-up stages), the columns are connected to a direct sequence without the additional heat integration. This is further optimized for minimum external heat demand. In subsequent steps, the superstructure model is refined to the direct sequence with heat integration. Afterwards an initial estimation of the pressure profile is performed using fixed F-factor values to ensure the numerical robustness of the model, after which the HETP and pressure drop correlations, as well as sizing and cost correlations are introduced to the model. After solving the extended model for minimum heat demand and total annualized cost, resulting in a fully initialized model with reasonable values for all variables, the binary decision variables are relaxed, and a minimization of the TAC is performed with successively increasing penalties until a MINLP solution is obtained. The sequence of model refinement and NLP solutions is performed automatically, such that the overall MINLP problem is started from an initial problem definition up to the final design, representing a proven (local) minimum of the cost objective, which satisfies the predefined product purities.

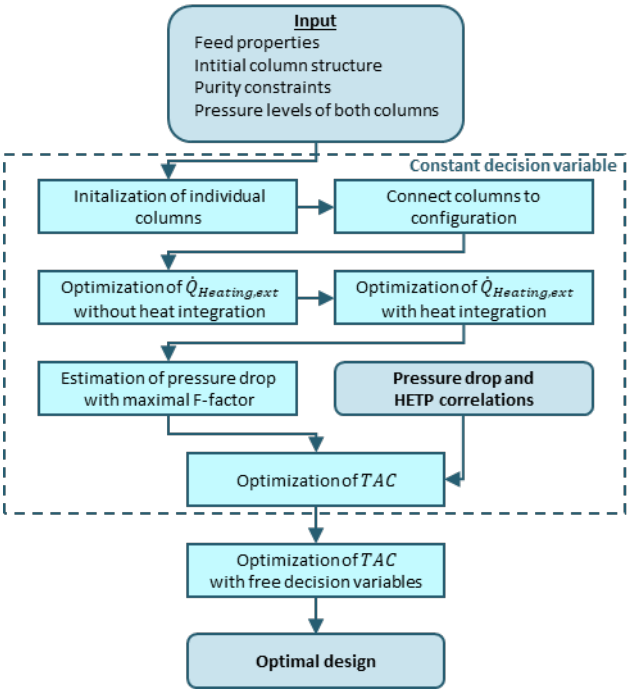

Figure 2. Initialization and solution procedure for direct heat integrated distillation sequence.

CASE STUDY AND RESULTS

To investigate the influence of stage-dependent pressure drop and HETP on the techno-economic design of heat-integrated direct distillation sequences, the separation of a saturated liquid feed into three product

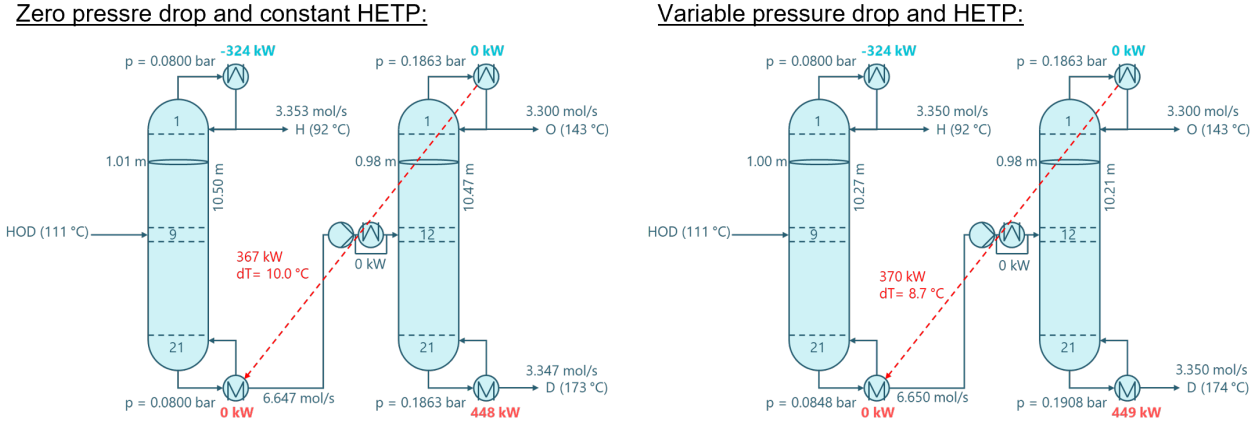

Figure 3. Optimalized heat-integrated direct distillation sequences for vacuum separation with isobaric (left) and pressure-drop-aware (right) superstructure.

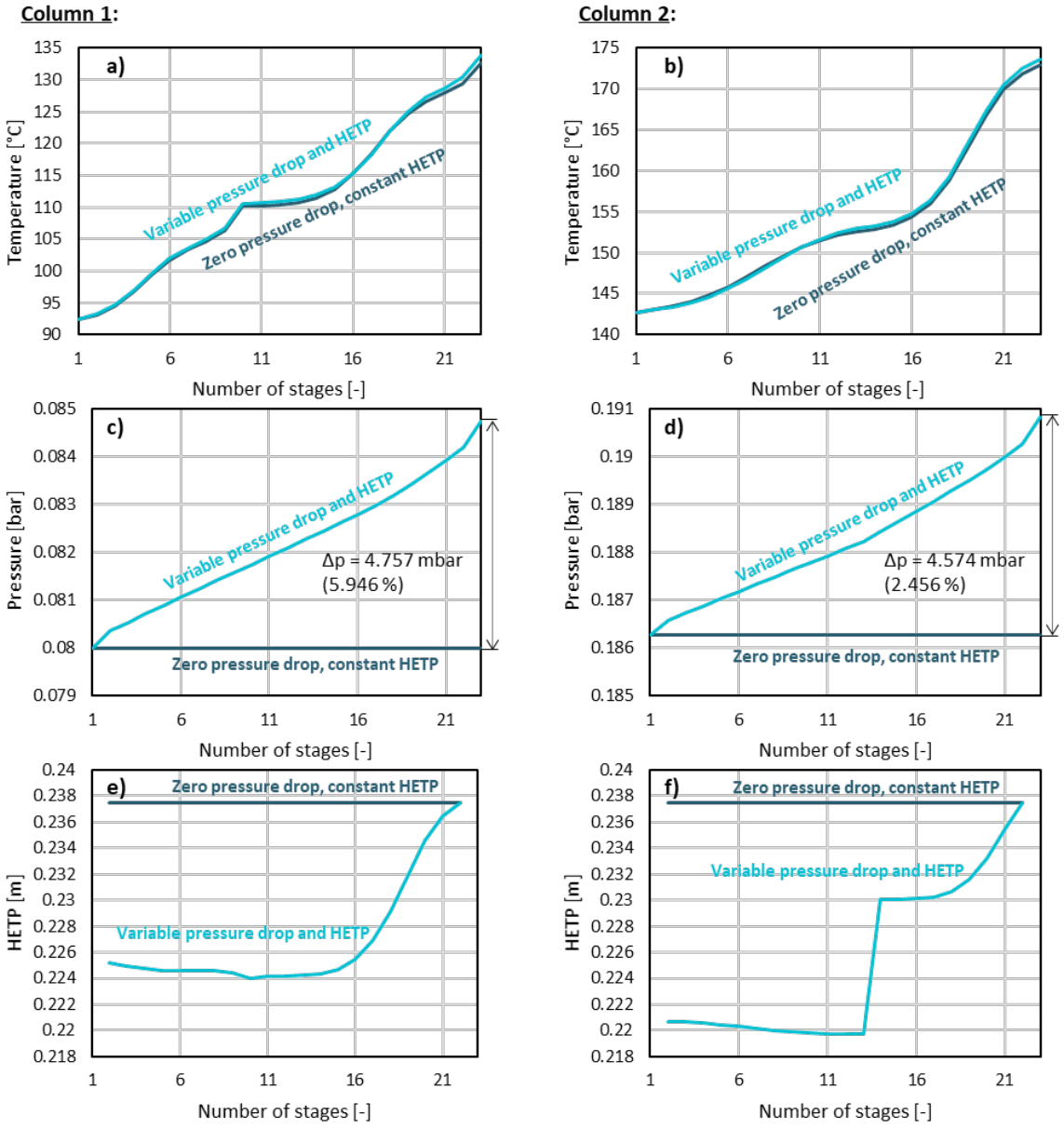

Figure 4. Temperature (a,b), pressure (c,d) and HETP (e,f) profiles inside of heat-integrated direct distillation sequence for vacuum separation with isobaric and pressure-drop aware superstructures.

streams with 99 mol% purity is considered.

The separation of hexanol, octanol, and decanol is investigated under vacuum conditions at 80 mbar [24], while the well-studied separation of benzene, toluene, and p-xylene is examined under atmospheric conditions [7, 19]. For both case studies, an equimolar feed and a feed flow rate of 10 mol/s are assumed. In the reference approach assuming isobaric columns with a constant HETP, the HETP is estimated for a maximum allowable F-factor of 1.75 $\sqrt{Pa}$ with the correlation stated in equation (5), resulting in a value of 0.238 m.

Cost data and economic assumptions are adopted from Adami et al. [19], while the VLE is modeled with the NRTL activity coefficient model and the Redlich-Kwong equation of state for the vapor phase fugacity. Pure component vapor pressure, heat capacities and heats of vaporization, are calculated with the extended Antoine equations and DIPPR correlations. All calculations are performed on an Intel i7-14700 CPU with GAMS 49.6.0 using SNOPT as NLP solver.

Influence on vacuum separation

The optimized flowsheets obtained from the

Table 1. Results of optimized flowsheet for atmospheric separation and vacuum separation with isobaric and pressure-drop-aware superstructure.

	Zero pressure drop, constant HETP		**Variable pressure drop and HETP**		**Relative difference**	
Vacuum separation:	Column 1	Column 2	Column 1	Column 2	Column 1	Column 2
Number of stages [-]	21	21	21	21	0%	0%
Column height [m]	10.50	10.47	10.27	10.21	-2.19%	-2.49%
Reboiler duty [kW]	366.65	448.01	370.21	448.88	+0.97%	+0.19%
Reboiler area [m²]	32.24	35.56	37.66	37.94	+16.81%	+6.69%
Bottom temperature [°C]	132.70	172.90	133.99	173.58	+0.97%	+0.39%
Bottom pressure [bar]	0.080	0.186264	0.0847568	0.190838	+5.95%	+2.46%
Temperature difference heat integration [K]	10.1		8.7		-13.86%	
Total annualized cost [k$/a]	285.324		286.417		+0.38%	
Atmospheric separation:	Column 1	Column 2	Column 1	Column 2	Column 1	Column 2
Number of stages [-]	28	44	28	44	0%	0%
Column height [m]	11.76	18.04	11.67	17.78	-0.78%	-1.47%
Reboiler duty [kW]	323.99	360.49	324.24	360.56	+0.08%	+0.02%
Reboiler area [m²]	28.23	14.03	29.05	14.19	+2.90%	+1.13%
Bottom temperature [°C]	122.65	161.37	122.93	161.61	+0.23%	+0.15%
Bottom pressure [bar]	1.01325	1.81977	1.02094	1.8304	+0.76%	+0.58%
Temperature difference heat integration [K]	10.1		9.8		-2.97%	
Total annualized cost [k$/a]	224.830		224.763		-0.03%	

optimization assuming isobaric operation and constant HETP and variable pressure drop and HETP are shown in **Figure 3**. Both approaches result in the same number of equilibrium stages in the optimal design. However, slight differences in the column height can be noticed. The variations are elucidated in **Figure 4**, which compares the resulting temperature profiles and highlights the variation in stage-specific pressure and HETP values for the resulting designs for both columns. While the temperature profiles are nearly identical, a slight increase in temperature toward the column bottom reduces the temperature difference for heat integration. Consequently, a considerable increase in the reboiler heat exchanger area is observed when pressure drop and HETP are included. Although the pressures increase almost linearly along the column height, which may also be reflected quite well with a constant stage specific pressure drop, the total pressure drop has no significant influence on the reboiler duty, which remains nearly unchanged between both approaches, indicating that isobaric operation and constant HETP can be appropriate approximations.

As the maximum F-factor, which determines the column diameter, occurs at the stage where the boil-up enters in both designs (cf **Figure 4**) the column diameter is basically equal for the two approaches. It is apparent that the HETP varies significantly between the rectifying and stripping sections, reflecting changes in vapor load along the column height and highlighting the importance for the resulting column sizing. This is also apparent in the key quantitative differences between the two designs, which are summarized in **Table 1**. Overall, it can be concluded that the consideration of column hydraulics does not show a significant effect on the energy demand and TAC, but has a noticeable effect on the HETP and the approach temperature in the heat exchanger. The latter might become more pronounced in case of a close boiling system, with higher stage requirements.

Influence on atmospheric separation

For the atmospheric separation, the qualitative trends observed in the vacuum case persist, but the impact of pressure drop is further reduced. As shown in **Table 1**, the relative pressure increase at the column bottom is below 1%, resulting in negligible effects on temperature profile, energy demand, and TAC.

However, analogous to the vacuum separation, the final column sizing is slightly influenced by the consideration of the stage-specific pressure drop and HETP values. In the context of the current investigation, the variations in investment cost exhibit no substantial influence on the overall TAC, as the operating costs are the prevailing factor in the objective function. In any case it is important to have a proper estimate of the pressure drop and HETP per tray to obtain a reliable estimate of the

column sizing and cost estimation.

Discussion and limitations

The current results indicate that the consideration of pressure drop and variable HETP can have a noticeable effect on the actual sizing of the column. However, the effect on the overall performance, in terms of heat duties and TAC, was limited for the wide boiling mixtures considered in the case studies. This indicates that assuming isobaric operation with constant HETP values is not expected to have a significant effect on the evaluation of competing configurations. While the overall economic impact is modest for the investigated wide-boiling mixtures, the effect may become larger for close-boiling or azeotropic mixtures and decreasing temperature differences for heat exchangers may become more decisive for thermally-coupled heat pump assisted distillation.

It also needs to be considered that the current proof-of-principle study applied simplified pressure drop and HETP correlations based on vendor data, which solely correlate with the F-factor. Consequently, variations in transport properties like liquid viscosity, surface tensions, as well as liquid load are not explicitly considered. Such effects may alter mass transfer efficiency and friction losses leading to a change in the correlation.

Nevertheless, the present implementation represents a first step towards incorporating pressure drop and variable HETP into an equation-oriented superstructure-optimization. It enables a more realistic assessment of structural design decisions at an early stage and provides valuable insights into the necessity of accounting for pressure-dependent effects in techno-economic optimization of energy-integrated distillation processes.

CONCLUSION

The presented extension of a superstructure-based optimization model for distillation processes by explicitly incorporating pressure drop and variable HETP values enables a systematic assessment of the influence of these effects on the techno-economically optimized grassroot design.

For the wide-boiling mixtures investigated, the inclusion of pressure drop and HETP correlations has only a minor impact on the overall energy demand and total annualized cost of heat-integrated direct distillation sequences. However, the results clearly indicate the effects on the specific sizing in terms of column height and heat exchanger areas. These effects become more pronounced under vacuum operation, where relative pressure changes along the column are significantly higher.

The presented case studies highlight that the relevance of pressure drop and stage-specific HETP strongly depends on the specific separation task and the chosen optimization objective. Consequently, these effects should be considered when evaluating alternative process configurations, especially in scenarios involving vacuum operation, close-boiling mixtures, or capital-intensive designs.

Future work will investigate the effect of the extension in the proposed approach for dividing wall columns, where vapor splits are inherently linked to pressure drop and column dimensions and heat pump assisted distillation. In addition, the robustness of different process alternatives with respect to multiple operating points and feed variation can be investigated. In order to account for changing properties, like viscosity and surface tension, and the liquid load over the column, generalized approaches, such as those proposed by Stichlmair et al. [25], will be incorporated and compared to the simplified, vendor-based correlations employed in the present study.

ACKNOWLEDGEMENTS

Funded by the Deutsche Forschungsgemeinschaft (DFG, German Research Foundation) – 523327609.

AUTHOR IDENTIFIERS

Author ORCIDs:
Betram S: 0009-0007-2326-469X
Schnurr J: 0009-0005-2907-8551
Skiborowski M: 0000-0001-9694-963X

REFERENCES

1. Oak Ridge National Laboratory. Materials for separation technologies, Energy Emiss. Reduct. Opport. (2005) https://doi.org/10.2172/1218755
2. Kiss AA, Smith R. Rethinking energy use in distillation processes for a more sustainable chemical industry. Energy 203:117788 (2020) https://doi.org/10.1016/j-energy.2020.117788
3. Blahušiak M, Kiss AA, Babic K, Kersten SRA, Bargeman G, Schuur B. Insights into the selection and design of fluid separation processes. Separation and Purification Technology 194:301-318 (2018). https://doi.org/10.1016/j.seppur.2017.10.026
4. Rix A, Hecht C, Paul N, Schallenberg J. Design of heat-integrated columns: industrial practice. Chemical Engineering Research and Design 147:83-89 (2019). https://doi.org/10.1016/j.cherd.2019.05.009
5. Waltermann T, Sibbing S, Skiborowski M. Optimization-based design of dividing wall columns with extended and multiple dividing walls for three- and four-product separations. Chemical Engineering and Processing - Process

Intensification 146:107688 (2019). https://doi.org/10.1016/j.cep.2019.107688
6. Ramapriya GM, Selvarajah A, Jimenez Cucaita LE, Huff J, Tawarmalani M, Agrawal R. Short-cut methods versus rigorous methods for performance-evaluation of distillation configurations. Ind. Eng. Chem. Res. 57:7726-7731 (2018). https://doi.org/10.1021/acs.iecr.7b05214
7. Adami M, Espert D, Skiborowski M. Rapid multi-criteria screening of energy-integrated distillation processes for nonideal mixtures. Sep. Purif. Technol. 377:134463 (2025) https://doi.org/10.15480/882.15774
8. Skiborowski M, Harwardt A, Marquardt W. Conceptual design of azeotropic distillation processes. Distillation :305-355 (2014). https://doi.org/10.1016/b978-0-12-386547-2.00008-9
9. Dejanovi? I, Matijaševi? L, Jansen H, Oluji? Ž. Designing a packed dividing wall column for an aromatics processing plant. Ind. Eng. Chem. Res. 50:5680-5692 (2011). https://doi.org/10.1021/ie1020206
10. Sangal VK, Kumar V, Mishra IM. Optimization of structural and operational variables for the energy efficiency of a divided wall distillation column. Computers & Chemical Engineering 40:33-40 (2012). https://doi.org/10.1016/j.compchemeng.2012.01.015
11. Barttfeld M, Aguirre PA, Grossmann IE. Alternative representations and formulations for the economic optimization of multicomponent distillation columns. Computers & Chemical Engineering 27:363-383 (2003). https://doi.org/10.1016/s0098-1354(02)00213-2
12. Jobson M. Energy considerations in distillation. Distillation :225-270 (2014). https://doi.org/10.1016/b978-0-12-386547-2.00006-5
13. Luyben WL. Effect of tray pressure drop on the trade-off between trays and energy. Ind. Eng. Chem. Res. 51:9186-9190 (2012). https://doi.org/10.1021/ie300634a
14. Li F, Luo Y, Yuan X. Equation-oriented optimization of a distillation column considering stage hydraulics. Ind. Eng. Chem. Res. 59:13657-13668 (2020). https://doi.org/10.1021/acs.iecr.0c01972
15. Horsch AS, Acevedo AR, Skiborowski M. Optimal Retrofit of Simple Distillation Sequences to Thermally Coupled Side-Stream Configurations. In: Proceedings of the 33rd European Symposium on Computer Aided Process Engineering. Ed: Kokssis A, Georgiadis MC, Pistikopoulos EN. Elsevier (2023) https://doi.org/10.1016/b978-0-443-15274-0.50053-6
16. Kraemer K, Kossack S, Marquardt W. Efficient optimization-based design of distillation processes for homogeneous azeotropic mixtures. Ind. Eng. Chem. Res. 48:6749-6764 (2009). https://doi.org/10.1021/ie900143e
17. Skiborowski M, Harwardt A, Marquardt W. Efficient optimization-based design for the separation of heterogeneous azeotropic mixtures. Computers & Chemical Engineering 72:34-51 (2015). https://doi.org/10.1016/j.compchemeng.2014.03.012
18. Waltermann T, Skiborowski M. Efficient optimization-based design of energy-integrated distillation processes. Computers & Chemical Engineering 129:106520 (2019). https://doi.org/10.1016/j.compchemeng.2019.106520
19. Adami M, Bertram S, Espert D, Skiborowski M. Beyond dividing wall columns: improved process intensification through liquid-only transfer and heat integration. Chemical Engineering and Processing - Process Intensification 218:110559 (2025). https://doi.org/10.1016/j.cep.2025.110559
20. Turton R, Bailie RC, Whiting WB, Shaeiwitz JA. Analysis, Synthesis, and Design of Chemical Processes. Prentice Hall PTR (2009)
21. Biegler LT, Grossmann IE, Westerberg AW. Systematic Methods of Chemical Process Design. Prentice Hall PTR (1997)
22. Douglas JM. Conceptual design of chemical processes. McGraw-Hill (1988)
23. Sulzer brochure for structure packings (accessed 26.01.2026). https://www.sulzer.com/en/-/media/files/products/separation-technology/brochures/english/structured_packings_e10686_en_web.pdf
24. Schnurr J, Adami M, Skiborowski M. Refrigerant selection and cycle design for industrial heat pump applications exemplified for distillation processes. Systems and Control Transactions 4:1306-1311 (2025). https://doi.org/10.69997/sct.119494
25. Stichlmair J, Bravo JL, Fair JR. General model for prediction of pressure drop and capacity of countercurrent gas/liquid packed columns. Gas Separation & Purification 3:19-28 (1989). https://doi.org/10.1016/0950-4214(89)80016-7